MedChemComm

Accepted Manuscript

ROYAL SOCIETY OF CHEMISTRY

www.rsc.org/medchemcomm

Cite this: DOI: 10.1039/c0xx00000x

www.rsc.org/xxxxxx

ARTICLE TYPE

Synthesis, characterization and evaluation of the substituent effect on the amoebicide activity of new hydrazones derivatives

Yanis Toledano[a†], Ruth Meléndrez Luévano[b], Marisol Navarro-Olivarria[b†], Juan Carlos García-Ramos[c], Marcos Flores-Alamo[c], Luis Ortiz-Frade[d], Lena Ruiz-Azuara[c], Blanca M. Cabrera-Vivas*[b].

Received (in XXX, XXX) Xth XXXXXXXXX 20XX, Accepted Xth XXXXXXXXX 20XX
DOI: 10.1039/b000000x

A series of 10 hydrazones were synthesized by the condensation of the selected hydrazine and the appropriate aldehyde. After the characterization and electrochemical analysis of each compound, amoebicidal activity was performed in vitro against the HM1: IMSS strain of *Entamoeba histolytica*. The results showed the influence of nitrobenzene group and the hydrazone linkage over the amoebicidal activity. Compound **1** present a promising amoebicidal activity with an IC50 = 0.98 µM, which represents a 7-fold increase in the potency of cell growth inhibition respect to metronidazole (IC_{50}= 6.8 µM). Moreover, compounds **2** and **4** present an amoebicidal activity comparable to the reference compound. These results show that the electronic environment of hydrazone derivatives reflected in redox potential values of the hydrazone linkage and nitro group play a fundamental role in the amoebicidal activity. Molecular structure of compound **1** was reported.

Introduction

Entamoeba histolytica is the parasite responsible for human amoebiasis, a disease characterized by extensive tissue destruction.[1] Amoebiasis is globally considered a leading parasitic cause of human mortality. About 10% of the world's population is affected by amoebiasis and approximately 40,000–100,000 deaths per year are related to this protozoan, mainly in developing countries.[2] Metronidazole and other nitroimidazole compounds are effective for the treatment of invasive amoebiasis but are less effective eliminating parasites located in the intestinal lumen. Several side effects were reported and go from vomiting and diarrhea to hallucinations,[3] besides the appearance of resistance strains to this drug.[4] While some authors still debate about whether or not metronidazole can induce encephalopathy,[5] the US National Toxicology Program indicates that " Metronidazole is *reasonably anticipated to be a human carcinogen* based on sufficient evidence of carcinogenicity from studies in experimental animals".[6] Therefore, new and better alternative therapies are required to control amoebiasis.

It has been reported that hydrazones present antidepressant,[7] anticonceptive,[8] and anticancer[9] activity. On the other hand, some derivatives have been assessed as antimicrobial[10] and bactericidal agents,[11] showing promising results against *Mycobacterium tuberculosis*[12] as well as in parasitic diseases such as leishmania[13], Chagas disease[14] and amebiasis.[15]

In this work it is reported the synthesis, characterization, electrochemical behavior and amoebicidal activity of 10 hydrazones sharing as a common feature, the hydrazone linkage. In these compounds, the substituent was modified to evaluate its influence over the amoebicidal activity. The results have shown a clear relationship of the amoebicidal activity with the redox potential of the evaluated molecules. The best amoebicidal activities have been shown by hydrazones with –nitro group as substituent.

Results and discussion

Synthesis

The synthesis of hydrazones derivatives consists in the condensation reaction of the selected hydrazine with the appropriate aldehyde as illustrated in scheme 1. Detailed reaction conditions can be consulted in our previous works.[16]

Molecular structure of compound 1.

The asymmetric unit consist of one molecule of compound 1 (1-((5-(4-nitrophenyl)furan-2-yl)methylene)-2-phenylhydrazine) that adopts an E configuration about the azomethine C═N double bond. Molecules are approximately planar with a N2-N1-C1-C6 torsion angle of 11.1(2)°. The furan ring makes dihedral angles of 1.2 (2) and 7.5 (2), respectively, with the methylidenehydrazine C═N─N plane and the benzene ring. The N-N distance [1.3580(17) Å] is similar than found in other hydrazones derived from phenylhydrazine such as (E)-1-(2-Nitrobenzylidene)-2-phenylhydrazine [1.349(2) Å] and (E)-1-(4-Methoxybenzylidene)-2-phenylhydrazine [1.3641(16) Å][17] and even similar to N-N distance found in compound 6 (*E*)-2-((5-(4-nitrophenyl)furan-2-yl)methylene)-1,1-diphenyl hydrazine [1.356(3) Å]. The N2=C7 double bond distance [1.285(2) Å] is in

Cite this: DOI: 10.1039/c0xx00000x

www.rsc.org/xxxxxx

ARTICLE TYPE

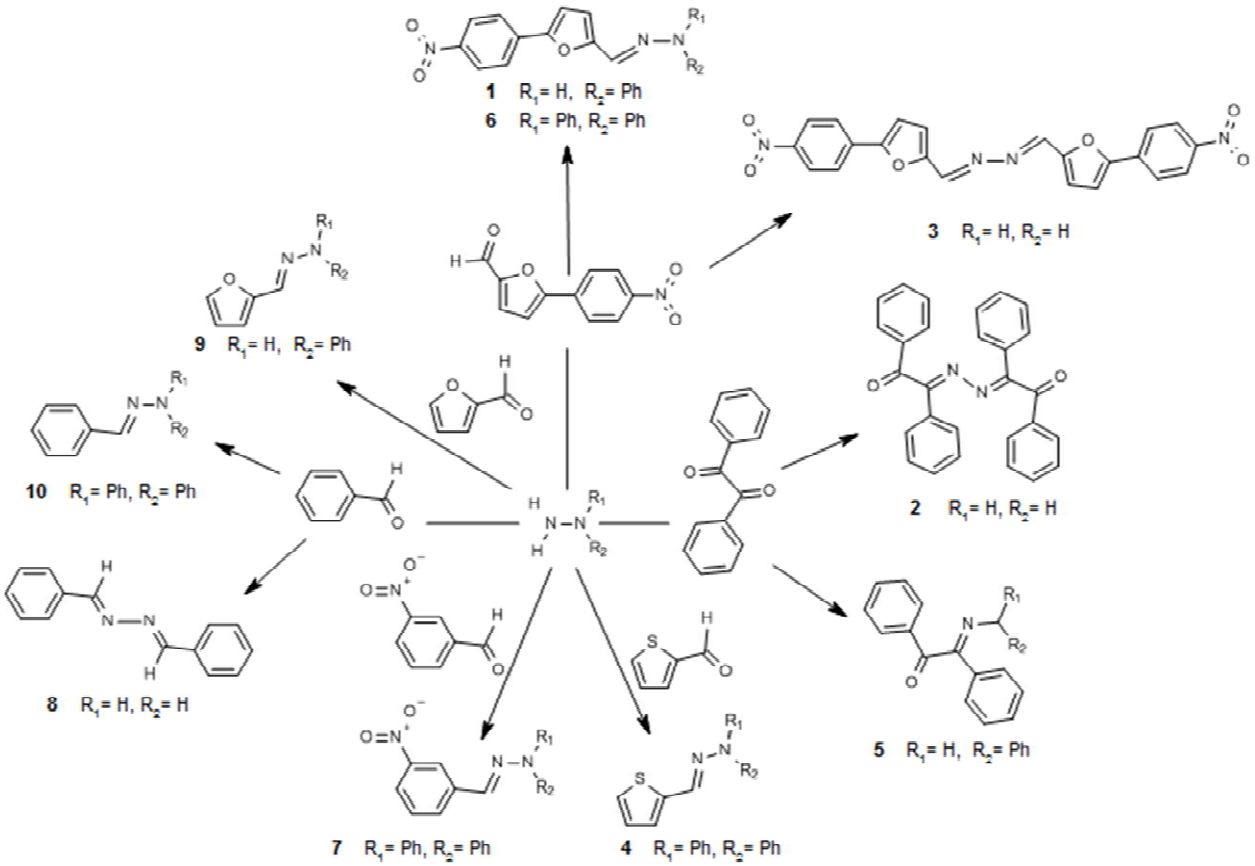

Scheme 1 General reaction pathway used to synthesize studied hydrazones. Syntheses were done in ethanol at room temperature.

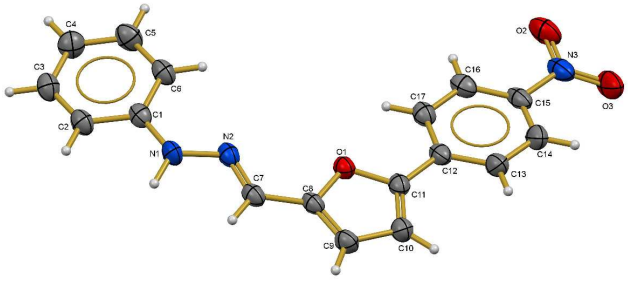

Fig. 1 Molecular structure of compound **1** (E)-1-((5-(4-nitrophenyl)furan-2-yl)methylene)-2-phenylhydrazine (50% probability level).

the range for a typical N=C bond distance [1.279(8) Å] reported by Allen.[18] The crystal packing shows N-H···O hydrogen bonds with interaction distance 3.0456(17) Å. Three of the molecules generates $R^3_3(37)$ rings. Molecular structure of compound **1** is shown in figure 1.

Electrochemical studies

Electrochemical behaviour was explored using cyclic voltammetry and square wave voltammetry. 1mM hydrazone in dimethylsulfoxide (DMSO) solution was used for all experiments. Figure 2 shows the typical cyclic voltammogram of compound **7** varying the switching potential $E_{+\lambda}$. When the potential scan was inverted at -1.289 V (Fig 2) one reduction signal I_c and, its corresponding oxidation signal I_a were observed. The ΔEp value near to 60 mV indicates a reversible electron transfer, attributed to the electrogeneration of the radical anion in the redox process R-NO_2 + 1e → R- $NO_2^{\bullet-}$.[19] On the other hand, when the potential was switched at -1.705 V one irreversible oxidation signal II_c was detected (Fig 2). This signal can be associated to one irreversible electron transfer with the cleavage of N-N bond follow by a proton release. From voltammogram presented in Fig 2 it can be also observed a change in the potential peak value and current peak value for signal I_a and the appearance of one oxidation process III_a. This behaviour is a consequence of the protonation of the radical anion in process I_a and the formation a new product in the process III_a. The absence of the corresponding oxidation signal for process II, lead us to use square wave voltammetry in order to obtain a parameter related

Table 1 Redox potential values of hydrazone linkage and nitrobenzene group. Inhibitory concentration values for compounds 1-10 against *E. Histolytica* cultures.

Compound	E_{IIc}[a] (V)	E_{Ic}[b] (V)	IC_{50} (μM)
1	-0.896	-0.425	0.98
2	-0.950	-----	18.0
3	-1.003	-0.658	13.0
4	-1.150	-----	7.6
5	-1.167	-----	47.0
6	-1.240	-0.725	16.0
7	-1.340	-0.739	19.0
8	-1.487	-----	96.0
9	-1.541	-----	120.0
10	-1.749	-----	78.0
Metronidazol	-----	-0.486	6.8

[a] Reduction peak potential values assigned to hydrazone linkage.[b] Redox potential values associated to nitrobenzene group. Redox potential values were referenced to NHE employing E_0= 0.640 V vs NHE for $Fc|Fc^+$ couple.

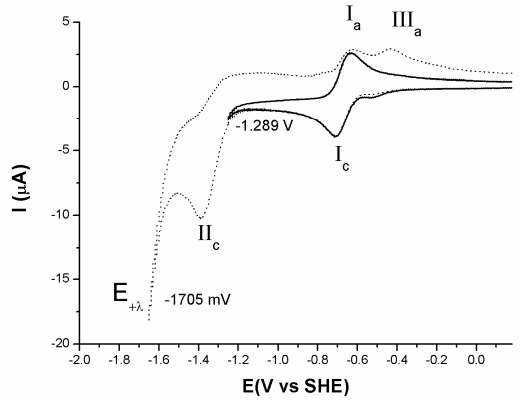

Fig. 2 Electrochemical behaviour of compound **7** studied in DMSO employing a platinum disk as a working electrode. Cyclic voltammogram scan rate 0.1 V/s.

with the reduction tendency of the studied hydrazones, that can be correlated with the biological activity observed, as discussed below. Reduction peak potential of the hydrazone linkage (IIc) and the nitrobenzene group when is present in the molecule (Ic) for compounds **1**-**10** are listed in table 1.

Amoebicidal activity

Metronidazole has become the drug of choice following recognition of its amoebicidal properties in the mid-1960s. Since then, nitroimidazole derivatives have been assayed as amoebicides and their activity is associated to the redox biotransformation of the nitro group that generates a short-lived nitroso free radical.[20] The production of reactive oxygen species (ROS) by nitroimidazoles has been proposed as the principal effect that leads to the elimination of the parasite, but the presence of super oxide dismutase (SOD) of *Entamoeba histolytica* induces a ROS regulation.[21] Moreover, resistance to metronidazole and other nitroimidazole compounds has been observed in the laboratory and clinically. The resistance mechanism has been investigated and is related to the down regulation of the pyruvate ferredoxin pathway in addition to stress mechanism including superoxide dismutase and peroxiredoxin.[22] This raises the need to generate compounds capable of producing a higher redox imbalance in the cell environment which produce several effects over the parasite.

Compound **1** has shown a high capacity to inhibit the proliferation of trophozoites of *Entamoeba histolytica* than the most used compound in the treatment of human amoebiasis, metronidazole. This compound presented an IC_{50}= 0.98 μM, which represent a 7-fold increase in the potency of cell growth inhibition respect to metronidazole (IC_{50}= 6.8 μM). While, compounds **3**, **6** and **7** with the presence of nitrobenzene group in their structures, have shown amoebicidal activities that can be considered acceptable with IC_{50} values of 13, 16 and 19 μM, respectively.

The high amoebicidal activity of compound **1** could be directly associated to the redox potential value of nitrobenzene moiety (E = -0.425V) which is lower than the observed for the nitro group of metronidazole, E = -0.486 V *vs* normal hydrogen electrode (NHE),[23] (table 1). The nitro group reduction redox potential values of compounds **1**, **3**, **6** and **7** have an inverse relationship with the amoebicidal activity as can be seen in figure 3a. As the reduction redox potential becomes more negative, a decrease in amoebicidal activity is observed. According to these results, it is patent that structural modifications producing a decrease of the reduction redox potential values for the nitro group leads to an increase of the amoebicidal activity. Comparing the structure of compounds **1** and **6** it is clear that the presence of a phenyl ring in the structure instead a hydrogen atom (R_1 in scheme 1) produces a difference of the redox potential of nitrobenzene moiety of 300mV. 3-nitrophenyl group instead the 4-nitrophenylfuran-2-yl generates almost the same difference of redox potential between compound **1** and **7**.

Compounds **2** and **4** also have important growth inhibition potency comparable with metronidazole, with IC_{50} of 18 and 7.6 μM respectively, even with the lack of nitro group in their structures. The amoebicidal activity of compound **4** could be related to the presence of the thiophene group in its structure. Thiophene can be oxidized to generate the sulfoxide derivatives, which have been already identified as highly reactive compounds[a] that could produce the parasite death through a redox imbalance mechanism different to that exerted by the compounds with nitrobenzene. Again, the structural modification is manifested comparing the amoebicidal activity of compound **4** with the showed by compound **9**, for the latter the thiophene group was substituted by a furan group with a 16-fold decrease of the amoebicidal activity.

Trying to explain the amoebicidal activity of compounds without the nitrobenzene group, we explore the influence of the hydrazine linkage over it. Recent reports suggest that the amoebicidal activity enhancement of hydrazone derivatives relies in the [-NH-N=CR_1R_2] linkage due their capacity to participate in the formation of hydrogen bonds.[15] Under our experimental conditions was possible to explore the electrochemical behaviour of the hydrazone linkage.

Amoebicidal activity presents a general tendency to decrease as the reduction redox potential for the hydrazone moiety increases (Fig 3b). Particular cases can be discussed taking into account the

Cite this: DOI: 10.1039/c0xx00000x

www.rsc.org/xxxxxx

ARTICLE TYPE

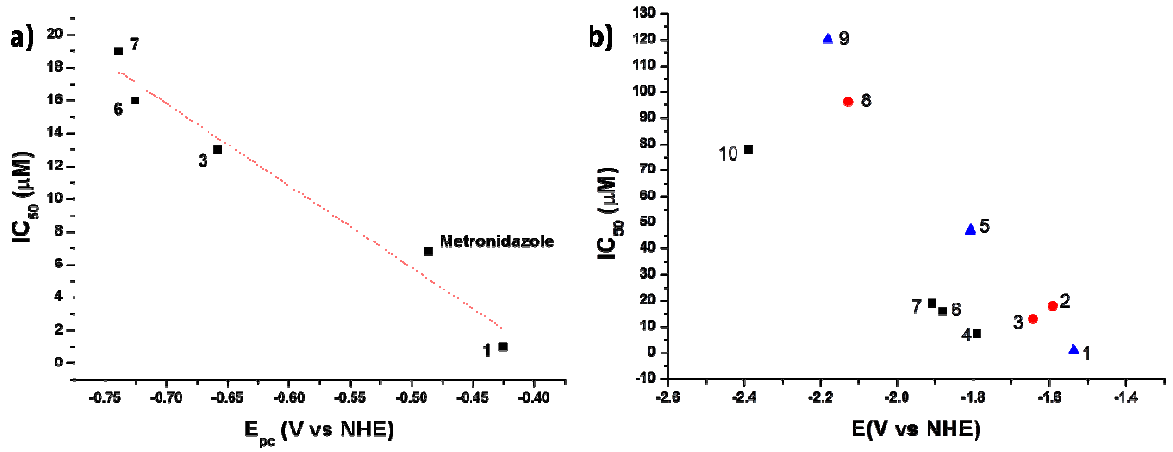

Fig. 3 Inverse relationship found for a) nitrobenzene redox potential values and amoebicidal activity, and b) reduction potential peak values of hydrazone linkage and amoebicidal activity of studied hydrazones **1**-**10**.

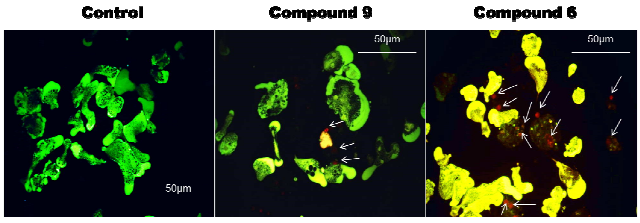

Fig. 4 Viability of *Entamoeba histolytica*. Cultures of *Entamoeba histolytica* treated with 1mM of compounds 9, and 6 stained with) carboxyfluorescein diacetate (CFDA) and propidium iodide (PI), 72h after administration. Shifting of green to yellowish fluorescent indicates decrease of viability. Nuclei of dead cells (white arrows).

different substituents in the molecules. Compounds **4**, **6**, **7** and **10** with two aromatic rings as substituents of the hydrazone present an inverse relationtioship between the reduction redox potential of the hydrazone and the IC_{50} in *E. histolytica* cultures. The equation that describes this behaviour is

$$IC_{50} = -208.05 - 119.59E_{IIc} \qquad R^2 = 0.9978 \quad (1)$$

The same behaviour is observed for compounds **1**, **5** and **9**. In this case the structure differs in one less aromatic ring as shown in scheme 1, and the equation that describe it is

$$IC_{50} = -185.17 - 284.98\ E_{IIc} \qquad R^2 = 0.9970 \qquad (2)$$

From equation 1 and 2, it can be established that structural modifications in the second group produce a higher effect on the biological activity, due to the coefficients that quantifies the contribution of the reduction redox potential. In this way it is interesting to note, that the effect of the hydrazone linkage over the biological activity present the same tendency as the one found on the nitro group reduction.

This effect can be appreciated comparing the reduction redox potential of the hydrazone linkage and the amoebicidal activities of compounds **1**, **3** and **6**. Compound **1** has the lowest redox potential (-0.896V) for this group as well as the lowest inhibitory concentration (0.98µM); followed by compound **3** (-1.003 V, 13 µM) and compound **6** (-1.240V, 16 µM). Other example without nitro group are compounds **2** and **5** where the former has a reduction redox potential of -0.95V and IC_{50} = 18µM and the latter -1.67V and IC_{50} = 47µM. Those could be extremely relevant because *Entamoeba histolytica* as other parasites do not possess the capacity to manage the redox imbalance produced by the hydrazone derivatives administrated to the culture.

Structural-activity relationship has been observed in 2-(quinolin-8-yloxy) acetylhydrazone derivatives which showed excellent amoebicidal activity compared to the cyclised products and is associated to the presence of quinolone nucleus and hydrazone linkage. In this case they have reported that the higher amoebicidal activity (0.03-0.08µM) was in compounds with a quinolone nucleus with a hydrazone linkage bearing a free N-H group. [15] Siddiqui and co-workers concluded that pyridil, azomethine group as well as the substituents, played a crucial role in amoebicidal activity. [21] It is reported too that the antileishmanial activity of 2-methoxybenzoylhydrazone mainly depends upon the presence of hydroxyl and methoxy groups and their respective position at the ring. [24]

Compound **6** which contents a nitro group in their structure presents and IC_{50} of 16µM, while compound **9** without a nitro group in their structure is the less active with an IC_{50} of 120µM;

which evinces again the importance of the substituents and the relevance of the nitro group in the amoebicidal activity of the hydrazones (Figure 4). Even though the number of evaluated compounds are not enough to realize a multivariable correlation to identify the contribution of the redox potentials over the amoebicidal activity ; using both redox potential values, nitrobenzene and hydrazone group, of compounds **1**, **3**, **6** and **7** produce the equation $IC_{50} = -5.4175\mathbf{E_{IIc}} - 47.2315\mathbf{E_{Ic}} - 23.8959$; n=4; $R^2 = 0.9708$; F= 50.93, where it is clear that the main component in the description of the amoebicidal activity of these compounds is the reduction redox potential of the nitrobenzene group, while the hydrazone linkage function is such as a secondary modulator, due the 10-fold lower value of its coefficient compared to the value that corresponds to the nitrobenzene group. However, these values have to be considered carefully.

Influence of hydrazone substituents on the amoebicidal activity of the compounds studied here can be appreciated comparing the redox potential and amoebicidal activity of compounds **1** and **6**. The phenyl group present in compound **6** generates an increase of 0.344 V in the reduction potential values for hydrazone linkage and 0.3 V for the reduction of nitro group, while the incorporation of 5-(4-nitrophenyl) furan-2-yl)methylene- moiety as a nitrogen substituent in compound **3** produces differences of 0.1 and 0.233 V for these groups respect to compound 1 (Table 1). The same effect is observed in the redox potential of the compound that does not possess the nitrobenzene moiety. The redox potential of the hydrazone linkage of compounds **2**, **5** and **8-10** is modified as a function of the substituent present. The presence of furan and phenyl ring produces the stabilization of the hydrazone linkage reflected in the energy employed for the reduction of this part of the molecule (compounds **8-10**), while the presence of electron withdrawing substituent such as carbonyl group produces the inverse effect (see Table 1). The increase of energy employed in the reduction of hydrazone group generates a decrease in the amoebicidal activity of the compounds evaluated in this work. Thus, differences in redox potential values are the responsible for the differences observed for the amoebicidal activity.

The behaviour observed in figure 3 between redox potential and the amoebicidal activity is also observed employing the chemical shift of the iminic proton of the hydrazones. Our results suggest that hydrazone linkage not only participates in the hydrogen bond formation but in redox processes too. This implies that amoebicidal activity of the studied hydrazones have to be related with the capacity of the molecule to distribute the electronic density over the whole molecule, which have a direct effect over the energy employed to reduce the nitro group, the hydrazone linkage and the generation of hydrogen bonds. Other analysis have to be done with the aim to determine the mechanism of hydrazones over the cultures of *Entamoeba histolytica* parasites, as well as cytotoxic evaluation because of hydrazones seems to be very good candidates as drugs to treat amoebiasis.

Conclusions

In this work is reported the synthesis, characterization and amoebicidal activity of ten new hydrazone derivatives. Compound **1** has shown a seven-fold increase in the amoebicidal activity than the first choice drug for human amoebiasis, metronidazole. Other five compounds, **2**, **3**, **4**, **6** and **7** have shown comparable growth inhibition capacity to metronidazole. Obtained results let us conclude that the electronic environment of the molecule is directly related with the amoebicidal activity. The most active compounds possess the nitrobenzene group in their structures. Our results shown that both reduction potential values, nitrobenzene and hydrazone linkage, are involved in the amoebicidal activity of these compounds. The former as the main actor while the latter function as a modulator of the amoebicidal activity. The activity shown by compound **4** is associated to the presence of thiophene group. Besides, the modulation of reduction redox potential due the modification of the substituents on the hydrazone linkage has to be exploited to find new amoebicidal agents.

Materials and methods

Chemistry

The hydrazones were synthesized by condensation reaction with the experimental conditions studied by our research group[16], briefly: 1.0 chemical equivalents of the corresponding hydrazine were dissolved in ethanol. A chemical equivalent of the desired aldehyde previously dissolved in the same solvent, was added drop by drop with continuous stirring. The reaction mixture was kept at room temperature and was monitored by TLC, and then vacuum filtered. The hydrazones were recrystallized and purified employing a chromatographic column. The hydrazones were characterized by mp, elemental analysis, UV-vis and IR spectroscopy, ^{1}H NMR, ^{13}C NMR, COSY, HSQC and in the case of compound **1** by X-ray diffraction.

UV were recorded on Varian Cary 50 Bio UV Visible spectrophotometer, IR (KBr) spectra were recorded on Nicolet FTIR Magna 750. Elemental analysis data were obtained in a Fisons Instruments Analyzer model EA 1108, using a sulfanilamide standard. ^{1}H NMR y ^{13}C NMR spectra were obtained on Varian VX-400 (400 MHz), chemical shifts were given on the delta scale as parts per million (ppm) with acetone d_6. Mass spectra were recorded on JEOL JEM JMS-SX 102 a 70 eV, data in mass/charge units (m/z). The reactants and the deuterated solvents were manufactured by the Aldrich Company and were used without further purification. The reactions were monitored by TLC, aluminum AlugramSil G/UV254 of 0.54 mm thickness.

(E)-1-((5-(4-nitrophenyl)furan-2-yl)methylene)-2-phenylhydrazine (1) Wine, borgoña crystals; yield: 75% at 25°C, mp. 175-176 °C. Anal. Calc. for $C_{17}H_{13}N_3O_3$ (M.W. = 307 gmol^{-1}) C, 66.4; H, 4.3; N, 13.7. Found: C, 66.6; H, 4.2; N, 13.7. $C_{17}H_{13}N_3O_3$ UV λ_{max} = 419 nm. FT. IR (film): (cm^{-1}): 3098 ν(C-H, Ph), 1586 ν(C=N), 1650-2000 ν(Ph). ^{1}H NMR (300 MHz, $(CD_3)_2CO$: (δ/ ppm, J/Hz):9.54 (s, 1H, NH), 8.27 (td, 2H, C3''), 7.93 (td, 2H, C2''), 7.78 (s, 1H, Ci), 7.24 (dd, 2H, C3',), 7.19 (d, 1H, 4'), 7.14 (dd, 2H, C2'), 6.82 (td, 1H, C4), 6.76 (d, 1H, C3). ^{13}C NMR (300 MHz, $(CD_3)_2CO$): (δ/ ppm): 153.10 (C5), 151.10 (C4'), 144.86 (C2), 135.97 (C1'), 129.11 (C3'), 126.26 (C=N),

124.29 (C3''), 123.82 (C2''), 119.73 (C4''), 113.25 (C1''), 112.37 (C2''),111.81 (C4), 111.02 (C3). MS-EI: m/z = 307 M^+.

(2E, 2'E)-2, 2'-(hydrazine-1, 2-diylidene) bis(1, 2-diphenylethanone) (2) Yellow solid; yield: 80% at 25°C, mp. 185-187 °C. Anal. Calc. for $C_{28}H_{20}N_2O_2$ UV λ_{max} = 382 nm. FT. IR (film): (cm^{-1}): 3125 ν(C-H, Ph), 1774 (C=O), 1680, ν(C=N), 710 ν (CH). ^{1}H NMR (300 MHz, $(CD_3)_2CO$: (δ/ ppm, J/Hz): 7.95(m, 4H, C2), 7.77 (m, 2H, C4), 7.63 (m, 8H, C3, C3'), 7.49 (m, 2H, C4'), 7.41 (m, 4H, C2'). ^{13}C NMR (300 MHz, $(CD_3)_2CO$): (δ/ ppm): 197.45 C1A, 167.05 (C2A), 135.41 (C1), 134.12 (C4), 132.12 (C1'), 131.72 (C4'), 129.17 (C3), 129.01 (C3'), 128.66 (C2),128.07 (C2'). MS-EI: m/z = 416 M^+.

(1E, 2E)-1, 2-bis- ((5-(4-nitrophenyl)furan-2-yl)methylene) hydrazine (3) Orange crystals; yield: 90% at 25°C, mp. 263-269 °C. Anal. Calc. for $C_{22}H_{14}N_4O_6$ (M.W. = 430 $gmol^{-1}$) C, 61.4; H, 3.3; N, 13. Found: C, 61.7; H, 3.42; N, 12.78.UV λ_{max} = 416 nm. FT. IR (film): (cm^{-1}): 3125 ν(C-H, Ph), 1574 ν(C=N), 1690-2000 ν(Ph). ^{1}H NMR (300 MHz, $(CD_3)_2CO$: (δ/ ppm, J/Hz): 8.19 (d, 2H, C3), 7.88 (d, 2H, C4), 7.49 (t, 4H, C3'), 7.27 (s, 2H, Ci), 7.26 (t, 4H, C2'). ^{13}C NMR (300 MHz, $(CD_3)_2CO$): (δ/ ppm): 146.90 (C4'), 143.08 (C5), 142.82 (C1'), 132.33 (C=N), 130.03 (C3'), 126.60 (C4), 125.35 (C2), 123.88 (C2'), 122.46 (C3). MS-EI: m/z = 430 M^+.

(E)-1, 1'-diphenyl-2-(thiophen-2-ylmethylene) hydrazine (4) Light Yellow crystals; yield: 75% at 25°C, mp. 117-119°C. Anal. Calc. for $C_{17}H_{14}N_2S$ (M.W. = 278 $gmol^{-1}$) C, 73.3; H, 5.1; N, 10.1. Found: C, 73.2; H, 5.0; N, 10.15. UV λ_{max}= 412 nm. FT. IR (film): (cm^{-1}): 3097 ν(C-H), 1667-1920 ν(Ph), 1585 ν(C=N), 1490 ν(C=C), 695 ν(C-S). ^{1}H NMR (400 MHz, $(CD_3)_2CO$: (δ/ ppm, J/Hz): 7.44 (m, 4H, C3'), 7.37 (d, 1H, C5), 7.36 (s, 1H, Ci), 7.21(m, 2H, C4'), 7.17 (dd, 4H, C2') 7.02(dd, 1H, C3), 6.98(dd, 1H, C4). ^{13}C NMR (300 MHz, $(CD_3)_2CO$): (δ/ ppm): 143.39 (C2), 141.67 (C1'), 130.52 (C5), 129.89 (C3'), 127.32 (C4), 127.01 (C3), 125.61 (C=N), 124.64 (C4'), 122.24 (C2'). MS-EI: m/z = 278.37M^+.

(2E, 2'E)-2,2'-(hydrazine-1,2-diylidene)bis(1,2-diphenylethanone) (E)-1,2-diphenyl-2-(2-phenylhydrazono)ethan-1-one (5) Yellow crystals; yield: 80% at 25°C. 158-161 °C. Anal. Calc. for $C_{20}H_{16}N_2O$ UV 210 nm λ_{max} = 210 nm. FT. IR (film): (cm^{-1}): 3098 ν(C-H, Ph), 1586 ν(C=N), 1650-2000 ν(Ph). ^{1}H NMR (300 MHz, $(CD_3)_2CO$: (δ/ ppm, J/Hz): 9.45 (s, 1H, NH), 8.02 (m, 2H, C2''), 7.59 (m, 2H, C4'), 7.53(m, 4H, C2', C3'), 7.47 (m, 1H, C4''), 7.42 (m, 2H, C3''), 7.22 (m, 2H, C3'''), 7.16 (m, 2H, C2'''), 6.92 (m, 1H, C4'''). ^{13}C NMR (300 MHz, $(CD_3)_2CO$): (δ/ ppm): 190.87 (C1), 143.87 (C1'), 142.01 (C1'''), 139.22 (C1''), 131.17 (C2''), 130.27 (C3'), 129.55 (C3''), 129.13 (C2'), 129.07 (C2), 129.00 (C4'), 127.61 (C4''), 121.83 (C4'''), 114.34 (C3''') 113.89 (C2'''). MS-EI: m/z = 300 M^+.

(E)-2-((5-(4-nitrophenyl)furan-2-yl)methylene)-1,1'-diphenyl hydrazine (6) Red crystals; yield: 78% at 25°C, mp. 163-165 °C. Anal. Calc. for $C_{23}H_{17}N_3O_3$ (M.W. = 383 $gmol^{-1}$) C, 72.1; H, 4.5; N, 11. Found: C, 72.3; H, 4.71; N, 10.90. UV λ_{max} = 415 nm. FT. IR (film): (cm^{-1}): 3119 ν(C-H, Ph), 1683, 1600 ν(C=N), 1667-2000, ν(Ph), 1513 ν_a(Ph-NO_2), 1221 ν(=C-O), 851 ν(PhNO_2). ^{1}H NMR (300 MHz, $(CD_3)_2CO$: (δ/ ppm, J/Hz): 8.23 (d, 2H, C3´, *J*= 8.88), 7.80 (d, 2H, C2' *J*= 8.88), 7.46 (dd, 4H, C3''), 7.22, (m, 6H, C2´,C4'), 7.06 (s, 1H, Ci), 6.91 (d, 1H, C4), 6.64 (d, 1H, C3). ^{13}C NMR (300 MHz, $(CD_3)_2CO$): (δ/ ppm): 153.49 (C4), 151.16 (C5), 146.14 (C2), 142.87 (C1'), 135.98 (C1''), 129.93 (C3''), 125.06 (C2''), 124.84 (C=N), 124.35 (C3'), 123.75 (C2'), 122.43 (C4''), 111.27 (C4), 110.76 (C3). MS-EI: m/z = 383 M^+.

(E)-2-(4-Nitrobenzylidene)-1,1'-diphenylhydrazine. (7) Yellow crystals, yield: 93% at 25°C, mp. 120-122°C. Anal. Calc. for $C_{19}H_{15}N_3O_2$ (M.W. = 317 $gmol^{-1}$) C, 71.9; H, 4.8; N, 10.3. Found: C, 72.1; H, 4.56; N, 12.93. UV λ_{max} = 411.51 nm. FT IR (film): (cm^{-1}): 3031 ν(C-H), 1591, 1556 ν(C=N), 1508 ν(Ph-NO_2). ^{1}H NMR (400 MHz, $(CD_3)_2CO$: (δ/ppm): 8.19 (m, 2H, C3), 7.87 (m, 2H, C6), 7.49 (m, 4H, C3'), 7.25 (m, 7H, C2', C4', Ci). ^{13}C NMR (400 MHz, $(CD_3)_2CO$): (δ/ ppm): 143.02 (C4), 143.01 (C1'), 142.80 (C1), 132.30 (C=N), 130.03 (C3'), 126.58 (C2), 125.35 (C4'), 123.88 (C3), 122.43 (C2'). MS-EI: m/z = 317 M^+.

(1E, 2E)-1,2-dibenzylidenehydrazine (8) Yellow crystals; yield: 81% at 25°C, mp. 85-89°C. Anal. Calc. for $C_{14}H_{12}N_2$ (M.W. = 208 $gmol^{-1}$) C, 80.7; H, 5.8; N, 13.5. Found: C, 80.4; H, 5.72; N, 13.20. UV λ_{max} = 313 nm. FT. IR (film): (cm^{-1}): 3125 ν(C-H, Ph), 1574 ν(C=N), 1690-2000 ν(Ph), 752, 691γ(CH). ^{1}H NMR (300 MHz, $(CD_3)_2CO$: (δ/ ppm, J/Hz): 8.67(s, 2H, Ci), 7.91 (m, 4H, C3), 7.50 (d, 4H, C2), 7.49 (d, 2H, C4). ^{13}C NMR (300 MHz, $(CD_3)_2CO$): (δ/ ppm): 161.56 (C=N),134.47 (C1),131.19 (C4),128.83 (C2),128.47 (C3). MS-EI: m/z = 208 M^+.

(E)-1-(furan-2-ylmethylene)-2-phenylhydrazine (9) Dark brown; yield: 70% at 25°C, mp. decomposition above 150 °C. Anal. Calc. for $C_{11}H_{10}N_2O$ (M.W. = 186 $gmol^{-1}$) C, 71.0; H, 5.4; N, 15. Found: C, 71.3; H, 5.15; N, 14.82. UV λ_{max} = 336.12 nm. FT. IR (film): (cm^{-1}): 3421 ν(N-H), 1452 ν(C=N). ^{1}H NMR (300 MHz, $(CD_3)_2CO$: (δ/ ppm, *J*/Hz): 9.66 (s, 1H, NH), 9.65 (s, 1H, C=N), 7.92 (m, 2H, C4, C3), 7.42 (d, 1H, C5), 7.41 (d, 2H, C2'), 6.73 (m, 3H, C3', C4'). ^{13}C NMR (300 MHz, $(CD_3)_2CO$): (δ/ ppm): 177.62 (C=N), 167.05 (C1'), 153.39 (C2), 148.52 (C2'), 121.43 (C5) , 121.42 (C3), 121.35 (C4), 114.50 (C4'), 112.61 (C3'). MS-EI: m/z = 186 M^+.

(E)-1-Benzylidene-2, 2'-diphenylhydrazine (10) Colorless crystals; yield: 79% at 25°C, mp. 116-118°C. Anal. Calc. for $C_{19}H_{16}N_2$ (M.W. = 272 $gmol^{-1}$) C, 83.8; H, 5.9; N, 10.3. Found: 83.4; 5.8; 9.95. UV λ_{max}= 340.13 nm. FT. IR (film): (cm^{-1}): 3060 ν(C-H, Ph), 2875 ν(H-C=N), 1586, 1490 ν(C=N).^{1}H NMR (300 MHz, $(CD_3)_2CO$: (δ/ppm, J/Hz): 7.64 (dd, 2H, C2), 7.46 (m, 4H, C3´), 7.35 (t, 2H, C3), 7.27 (1H, C4), 7.22 (m, 6H, C2´,C4´), 7.18 (s, 1H, Ci). ^{13}C NMR (300 MHz, $(CD_3)_2CO$): (δ/ ppm): 144.49 (C1), 137.08 (C1´), 136.00 (C=N), 130.68 (C3), 129.36 (C3'), 128.92 (C4), 126.99 (C2), 125.39 (C4'), 123.16 (C2'). MS-EI: m/z = 272 M^+.

Single crystal X-ray crystallography. Crystal of compound **1** mounted on glass fiber were studied with a Oxford Diffraction Gemini "A" diffractometer with a CCD area detector, with radiation source of $\lambda_{CuK\alpha}$= 1.5418 Å using graphite-monochromatized radiation. CrysAlisPro and CrysAlis RED software packages[25] were used for data collection and data

integration. A data sets consisted of 1190/19 frames/runs of intensity data collected with a frame width of 1° in ω, a counting time of 1.0 to 2.8 s/frame, and a crystal-to-detector distance of 55.00 mm. The double pass method of scanning was used to exclude any noise. The collected frames were integrated by using an orientation matrix determined from the narrow frame scans. Final cell constants were determined by a global refinement; collected data were corrected for absorbance by using Analytical numeric absorption correction[26] using a multifaceted crystal model based on expressions upon the Laue symmetry using equivalent reflections.

Structure solution and refinement were carried out with the program(s): SHELXS97[27]; SHELXL97; for molecular graphics: ORTEP-3 for Windows[28]; and the software used to prepare material for publication: WinGX 1.80.05[29].

Full-matrix least-squares refinement was carried out by minimizing $(Fo^2 - Fc^2)^2$. All non-hydrogen atoms were refined anisotropically; The H atoms of the amine group (H-N) were located in a difference map and refined isotropically with U_{iso}(H) = 1.2 U_{eq}. H atoms attached to C atoms were placed in geometrically idealized positions and refined as riding on their parent atoms, with C—H = 0.95 A ° and with U_{iso} (H) = 1.2U_{eq}(C) for aromatic groups. Crystal data and experimental details of the structure determination are listed in Table 1.

The crystallographic data for the structure reported in this paper have been deposited with the Cambridge Crystallographic Data Centre as supplementary publication no. CCDC-986296. Copies of the data can be obtained free of charge on application to CCDC, 12 Union Road, Cambridge, CB2 1EZ, UK (fax: (+44) 1223-336-033, e-mail: deposit@ccdc.cam.ac.uk).

Electrochemical measurements. All electrochemical studies were performed at sample concentrations of ca. 1 mM in the presence of DMSO containing 0.1 M tetra-N-butylammonium hexafluorophosphate ($TBAPF_6$), using a potentiostat/galvanostat EG&G PAR 263A. A typical three electrode array was employed. The working electrode was a platinum disk. A platinum wire served as a counter-electrode and a silver wire was used as a pseudo-reference electrode. All solutions were bubbled with nitrogen 10 min prior to each measurement. Cyclic voltammetry experiments were initiated from open circuit potential (E_{ocp}), using a scan rate of 0.1 V s−1 in negative and positive direction. As an internal reference ferrocene was added at the end of each set of experiments. All potentials were reported versus the couple Fc/Fc+ according to the IUPAC convention. Square wave voltammetry experiments were acquired with amplitude of 25 mV using a frequency of 100 Hz. Positive feedback method was used for iR compensation during all the experiments.

Biology

Amoebicidal activity. *E. histolytica* HM1-IMSS trophozoites were axenically grown in TYI-S33 medium.20 Amoebas (1 × 105 of live trophozoites) were placed in tubes with 3 ml TYI-S33 supplemented with each compound so that the final concentrations were as follows: 1000, 100, 10, 1 and 0.1 µM.

Amoebic trophozoites viability was assessed employing two different methods, (1) vital marker trypan blue and (2) carboxyfluorescein diacetate (CFDA) and propidium iodide done at 24, 28 and 72 hours under a microscope using a haemocytometer. In brief, samples of 100 µl containing around 1 × 104 treated parasites were added with 100 µl trypan blue 0.4% or 1 µl of 5 µM CFDA (Invitrogen, USA) and 1 µl of 1.5 µM propidium iodide, mixed and incubated at room temperature for 15 min. Viable cells were counted using the fluorescent microscope Olympus BX51.

Acknowledgements

The authors thank VIEP-BUAP (CAVB-NAT-G13 and MELR-NAT-G13), CONACyT (130500, 179119, and 194130), UNAM-PAPIIT (217613) and UNAM-PAIP (3590-19) for financial support. YTM and JCGR thank CONACyT for the scholarship.

Notes and references

[a] *Departamento de Inmunología, Instituto de Investigaciones Biomédicas, Universidad Nacional Autónoma de México. Av. Universidad 3000, CU, 04510, Mexico City, Mexico.*
[b] *Departamento de Química Orgánica, Facultad de Ciencias Químicas, Benemérita Universidad Autónoma de Puebla. 72570, Puebla, Pue., Mexico.*
[c] *Departamento de Química Inorgánica y Nuclear, Facultad de Química, Universidad Nacional Autónoma de México, Avenida Universidad 3000, 04510 Mexico City, Mexico.*
[d] *Electrochemistry Department, Centro de Investigación y Desarrollo Tecnológico en Electroquímica S.C. Parque Tecnológico Querétaro, Sanfandila, Pedro de Escobedo, C.P. 76703 Querétaro, México.*

† Electronic Supplementary Information (ESI) available: Bond distances, angles and details of data colection and refinement can be consulted in the supplementary information. See DOI: 10.1039/b000000x/

‡ Footnotes should appear here. These might include comments relevant to but not central to the matter under discussion, limited experimental and spectral data, and crystallographic data.

1 H. Brandt and R. Pérez-Tamayo, *Hum. Pathol.* 1970, **1**, 351.
2 S.L. Stanley Jr., *Lancet*, 2003, **361**, 1025; R. Fotedar, D. Stark, N. Beebe, D. Marriot, J. Ellis and J. Harkness, *Clin. Microbiol. Rev.* 2007, **20**, 511
3 P. L. Johanson, *Parasitol. Today*, 1993, **9**, 183.
4 P. Goldman, R. L. Koch, T. C. Yeung, E. J. Chrystal, B. B. Beaulieu Jr., M. A. McLafferty, and G. Sudlow, *Biochem. Pharmacol.*, 1986, **35**, 43.
5 D. Kim, J. Park, B. Yoon, M.J. Baek, J.E. Kim and S.Y. Kim, *J. Neurol. Sci.* 2004, **224**, 107; *Indian J Pharmacol.* 2013, **45,** 295; A. Kuriyama, J.L. Jackson, A. Doi and T. Kamiya, *Clin. Neuropharmacol.* 2011, **34,** 241.
6 *Rep. Carcinog.* 2011, **12**, 269.
7 F. Chimenti, E. Maccioni, D. Secci, A. Bolasio, P. Chimenti, A. Granese, O. Bofani, P. Turini, S. Alcaro, F. Ortuso, M.C. Cardia and S. Distinto, *J. Med. Chem.* 2007, **50**, 707; K. Navakovski de Oliveira, P. Costa, J. R. Santin, L. Mazzambani, C. Bürger, C. Mora, R.J. Nunes and M. M. de Souza, *Bioorg. Med. Chem.* 2011, **19**, 4295; O.D. Can, M.D. Altintop, U.D. Ozkay, U.I. Uçel, B. Doğruer and Z.A. Kaplancikli, *Arch. Pharm. Res.* 2012, **35**, 659.
8 R. B. Lacerda, L. L. da Silva, C. K. F. de Lima, E. Miguez, A. L. P. Miranda, S. A. Laufer, E. J. Barreiro and C. A. M. Fraga, *PLoS ONE,* 2012, **7**, e46925; K. N. de Oliveira, M. M. Souza, P. Cunha Sathler, U. O. Magalhães, C. R. Rodrigues, H. C. Castro, P. R. Palm, M. Sarda, P. E. Perotto, S. Cezar, M. A. de Brito, A. S. S. R. Ferreira, L. Mendes Cabral, C. Machado and R. J. Nunes, *Arch. Pharm. Res.* 2012, **35**, 1713; C.D. Duarte, J. L. Tributino, D. I. Lacerda, M. V. Martins, M.S. Alexandre-Moreira, F. Dutra, E. J. Bechara, F. S. De-Paula, M.O. Goulart, J. Ferreira, J. B. Calixto, M. P. Nunes, A.L.

Bertho, A.L. Miranda, E. J. Barreiro and C. A. Fraga, *Bioorg. Med. Chem.* 2007, **15**, 2421.
9 P. Kumar, B. Narasimhan, *Mini Rev. Med. Chem.* 2013, **13,** 971; Z. Cui, Y. Li, Y. Ling, J. Huang, J. Cui, R. Wang and X. Yang, *Eur. J. Med. Chem.* 2010, **45**, 5576; K. S. Putt, G. W. Chen, J. M. Pearson, J. S. Sandhorst, M. S. Hoagland, J.-T. Kwon, S.-K. Hwang, H. Jin, M. I. Churchwell, M.-H. Cho, D. R. Doerge, W. G. Helferich and P. J. Hergenrother, *Nat. Chem. Biol.* 2006, **2**, 543.
10 A. M. Pieczonka, A. Strzelczyk, B. Sadowska, G. Mlostoń and P. Stączek, *Eur. J. Med. Chem.* 2013, **64**, 389; P. Kodisundaram, S. Amirthaganesan and T. Balasankar, *J. Agric. Food Chem.* 2013, 61, 11952; H. G. Aslan, S. Özcan and N. Karacan, *Spectrochim. Acta A Mol. Biomol. Spectrosc.* 2012, **98**, 329.
11 C. Chen, N. K. Dolla, G. Casadei, J. B. Bremner, K. Lewis and M. J. Kelso, *Bioor. Med. Chem.* 2014, **24**, 595.
12 U. A. More, S. D. Joshi, T. M. Aminabhavi, A. K. Gadad, M. N. Nadagouda and V. H. Kulkarni, *Eur. J. Med. Chem.* 2014, **71**, 199; F.R. Pavan, P.I. da S. Maia, S. R. Leite, V. M. Deflon, A.A. Batista, D. N. Sato, S. G. Franzblau and C. Q. Leite, *Eur. J. Med. Chem.* 2010, **45**, 1898.
13 E. S. Coimbra, L. M. R. Antinarelli, A. D. da Silva, M. L. F. Bispo, C. R. Kaiser and M. V. N. de Souza, *Chem. Biol. Drug Des.* 2013, **81**, 658; M. Taha, M. S. Baharudin, N. H. Ismail, K. M. Khan, F. M. Jaafar, Samreen, S. Siddiqui and M. I. Choudhary, *Bioog. Med Chem. Lett.* 2013, **23**, 3463.
14 D.R. Moreira, A.C. Lima Leite, M.V. Cardoso, R.M. Srivastava, M.Z. Hernandes, M.M. Rabello, L.F. da Cruz, R.S. Ferreira, C.A. de Simone, C.S. Meira, E.T. Guimaraes, A.C. da Silva, T.A. Dos Santos, V.R. Pereira and M.B. Pereira Soares, *ChemMedChem* 2014, **9**, 177; P. Hernández, R. Rojas, R.H. Gilman, M. Sauvain, L.M. Lima, E.J. Barreiro, M. González and H. Cerecetto, *Eur. J. Med. Chem.* 2013, **59**, 64.
15 F. Hayat, A. Salahuddin, J. Zargan, A. Azam, *Eur. J. Med. Chem.* 2010, **45**, 6127; S. M. Siddiqui, A. Salahuddin, A. Azam, *Eur. J. Med. Chem.* 2012, **49**, 411.
16 R. Meléndrez-Luévano, B. M. Cabrera-Vivas, M. Flores-Alamo, J.C. Ramírez and P. Conde-Sánchez, *Acta Cryst. E.* 2013, **69**, o1039; M. Flores-Alamo, B.M. Cabrera-Vivas, R. Meléndrez-Luevano, J. M. Hernández P. and L. Ruiz-Azuara, *Acta Cryst. E.* 2013, **69**, o90; A. Mendoza, R. Meléndrez-Luévano, B.M. Cabrera-Vivas, C. Acoltzi-X and M. Flores-Alamo, *Acta Cryst. E.* 2012, **68**, o3238; A. Mendoza, R. Meléndrez-Luévano, B.M. Cabrera-Vivas, C.D. Lozano-Márquez and V. Carranza, *Acta Cryst. E*, 2012, **68**, o434; A. Mendoza, B.M. Cabrera-Vivas, R. Meléndrez-Luévano, J.C. Ramírez and M. Flores-Alamo, *Acta Cryst. E,* 2011, **67**, o1287; A. Mendoza, B.M. Cabrera-Vivas, R. Meléndrez-Luévano, J.C. Ramírez and M. Flores-Alamo, *Acta Cryst. E*, 2010, **66**, o2349; A. Mendoza, B.M. Cabrera-Vivas, R. Meléndrez-Luévano, T. Pacheco-Álvarez and V. Carranza, *Acta Cryst. E,* 2010, **66**, o2058.
17 H.A. Shad, M.N. Tahir, M.I. Tariq, M. Sarfraz and S. Ahmad *Acta Cryst. E* 2010, **66**, o1955; M. Mufakkar, M.N. Tahir, M.I. Tariq, S. Ahmad and M. Sarfraz *Acta Cryst. E* 2010, **66**, o1887.
18 F.H. Allen, O. Kennard, D.G. Watson, L. Bammer, G. Orpen and R. Taylor *J. Chem. Soc., Perkin Trans. 2* 1987, S1.
19 J.A. Fry, The Electrochemistry of nitro, nitroso, and related compounds, in: S. Patai (Ed.), The Chemistry of Amino, Nitroso, Nitro and Related Groups, Supplement F2, John Wiley and Sons, Ltd., New York, 1996.
20 B.L. Tekwani, R.K. Mehlotra, *Microbes Infect.* 1999, **1**, 385.
21 D. G. Lindmark, M. Muller, Antimicrobial agents and chemotherapy, 1976, 476-482
22 S.M. Siddiqui, A. Salahuddin, A. Azam, *Eur. J. Med. Chem.* 2012, 49, 411.
23 A. Dhand, D.R. Snydman, Mechanism of Resistance in Metronidazole in: Mayers D.L. (Ed.), Antimicobial Drug Resistance: Mechanism of Drug Resistance. Vol. 1, Humana Press, New York, 2009
A D.R. Hawkings in Comprehensive Medicinal Chemistry II, Volume 5 (Eds. J.B. Taylor, D.J. Triggle) Elsevier, Amsterdam, 2007, Pp. 800.
24 M. Taha, M.S. Baharudin, N.H. Ismail, K.M. Khan, F. M. Jaafar, S.S. Siddiqui, M. I. Choudhary, *Bioorg. Med. Chem. Lett.* 2013, **23**, 3463.
25 Oxford Diffraction (2007). CrysAlis CCD and CrysAlis RED. Oxford Diffraction Ltd, Abingdon, England.
26 R.C. Clark and J.S. Reid *Acta Cryst. A* 1995, **51**, 887.
27 G.M. Sheldrick, (2008). SHELXS97 and SHELXL97. University of Gottingen, Germany.
28 L.J. Farrugia, *J. Appl. Cryst.* 1997, **30**, 565.
29 L.J. Farrugia, *J. Appl. Cryst.* 1999, **32**, 837.

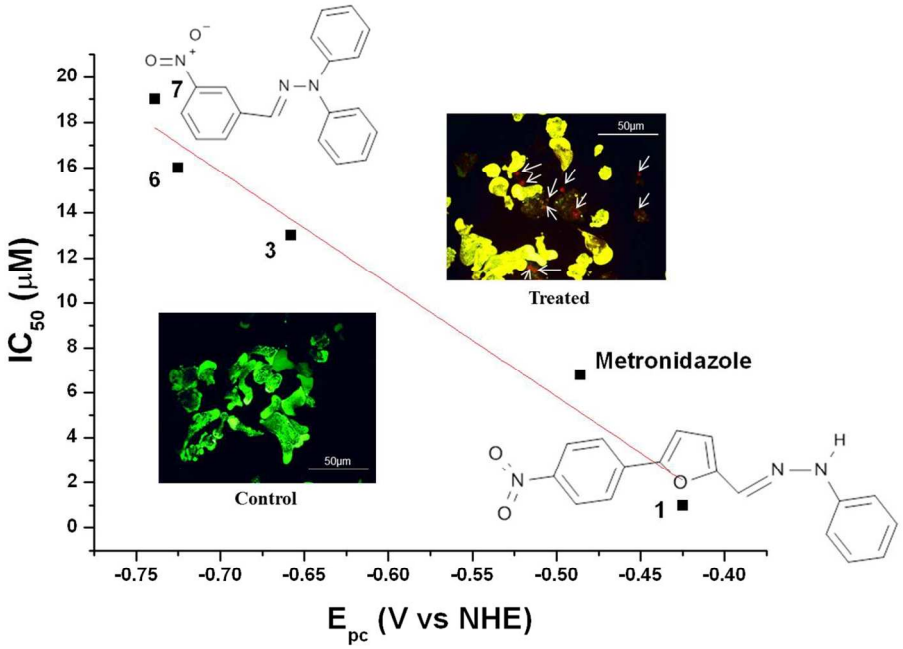

The electronic environment of hydrazone derivatives reflected in redox potential values of the hydrazone linkage and nitro group play a fundamental role in the amoebicidal activity.
254x175mm (150 x 150 DPI)

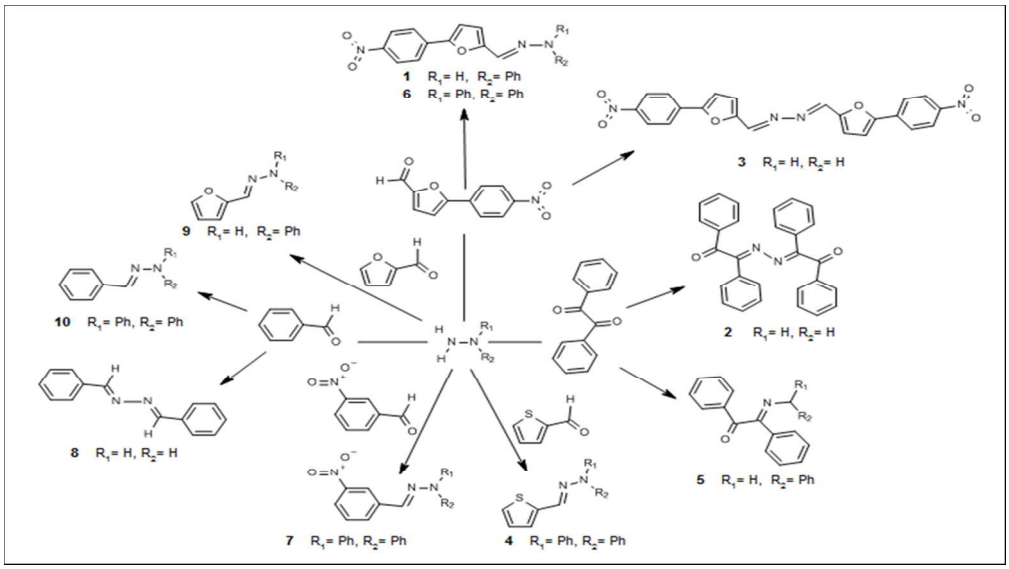

Scheme 1. General reaction pathway used to synthesize studied hydrazones. Syntheses were done in ethanol at room temperature.
250x172mm (139 x 113 DPI)

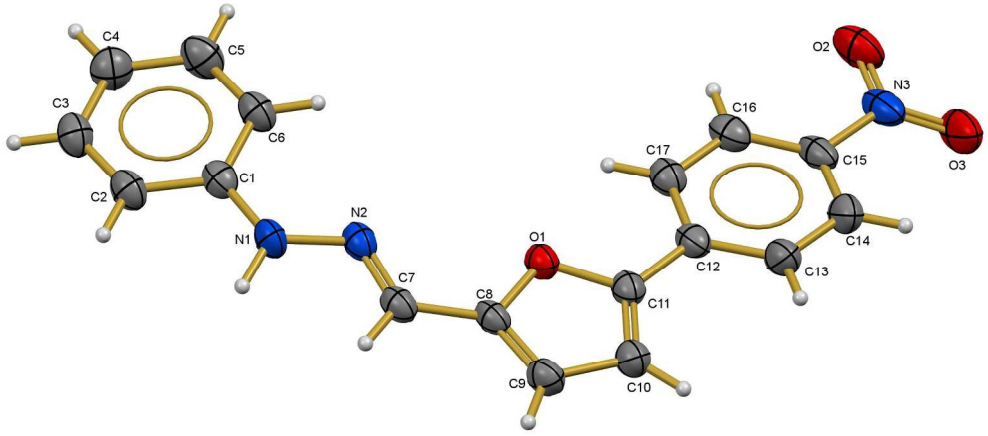

Fig 1. Molecular structure of compound 1 (E)-1-((5-(4-nitrophenyl)furan-2-yl)methylene)-2-phenylhydrazine (50% probability level).
623x291mm (96 x 96 DPI)

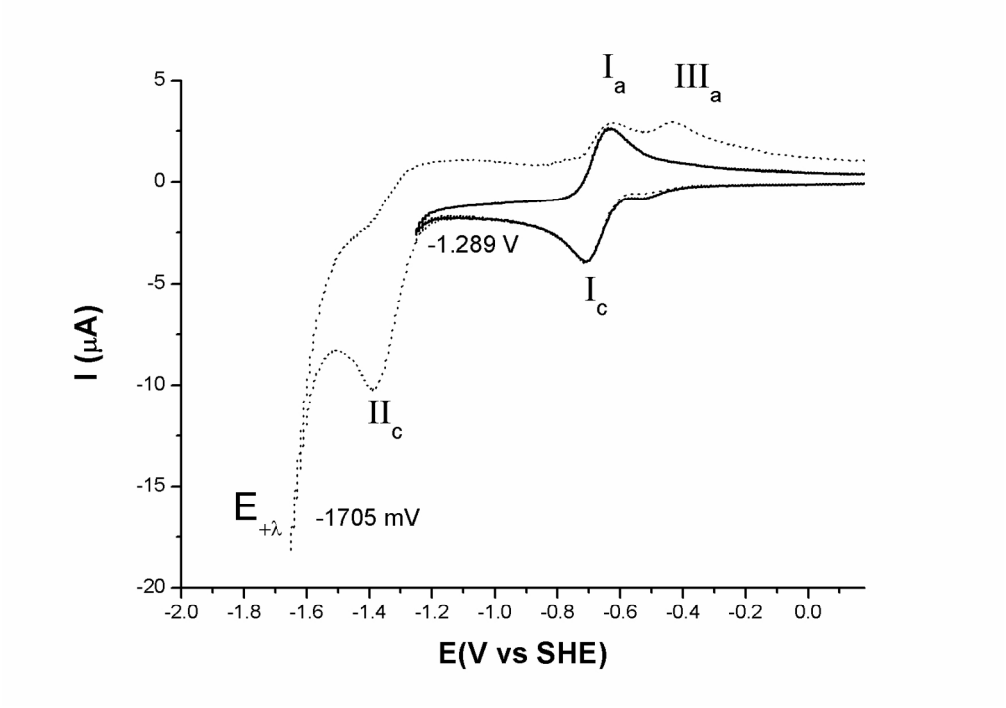

Fig. 2 Electrochemical behaviour of compound 7 in DMSO employing a platinum disk as a working electrode. Cyclic voltammogram 100 mV/s.
297x209mm (150 x 150 DPI)

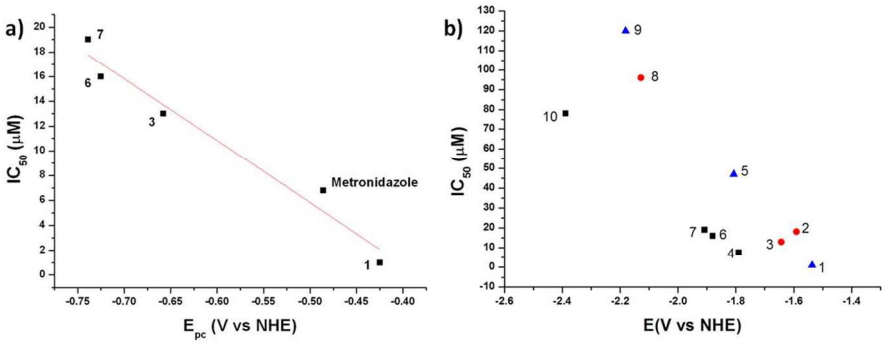

Fig. 3 Inverse relationship found for a) nitrobenzene redox potential values and amoebicidal activity, and b) reduction potential peak values of hydrazone linkage and amoebicidal activity of studied hydrazones 1-10.
254x98mm (150 x 150 DPI)

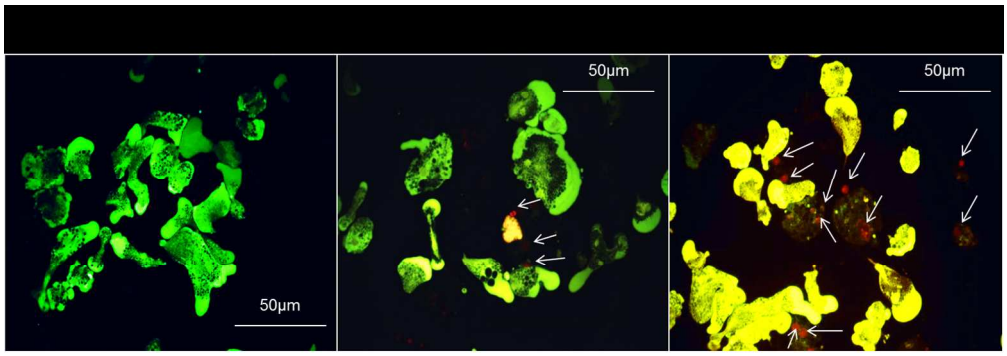

Fig. 4. Viability of Entamoeba histolytica. Cultures of Entamoeba histolytica treated with 1mM of compounds 9, 6, 3 stained with CFDA and PI, 72h after administration. Shifting of green to yellowish fluorescent indicates decrease of viability. Nuclei of dead cells (white arrows).
264x91mm (150 x 150 DPI)